Current Research in Food Science 5 (2022) 1158–1166

Contents lists available at ScienceDirect

Current Research in Food Science

journal homepage: www.sciencedirect.com/journal/current-research-in-food-science

Electrochemical determination of synephrine by using nafion/UiO-66/graphene-modified screen-printed carbon electrode

Yi Zhang, Zongyi You, Liangliang Liu *, Shengwen Duan ***, Aiping Xiao **

Institute of Bast Fiber Crops, Chinese Academy of Agricultural Sciences, Changsha, 410205, China

ARTICLE INFO

Handling Editor: Professor A.G. Marangoni

Keywords:
Graphene
Screen-printed electrode
Sensor
Synephrine
UiO-66

ABSTRACT

The screen-printed carbon electrode (SPCE) was one step modified with graphene (GN) and UiO-66 composites in nafion solution as a portable sensor (nafion/UiO-66/GN/SPCE) for the detection of synephrine. The used GN and UiO-66 were well-characterized, exhibiting typical structures by scanning electron microscope (SEM) with energy dispersive spectroscopy (EDS), X-ray powder diffraction (XRD), and Fourier transform infrared spectroscopy (FTIR). The nafion/UiO-66/GN/SPCE showed the maximum electrochemical signals for synephrine when comparing fabricated components in the cyclic voltammetric method. It was systematically investigated in modifier composition, modification volumes, pH, scan rate, and quantitative analysis ability. Under optimal conditions, the sensor exhibited a good detection limit (0.04 μmol L^{-1}) for synephrine with a linear range of 0.5 μmol L^{-1} to 60 μmol L^{-1} ($r^2 = 0.995$). The nafion/UiO-66/GN/SPCE had adequate reproducibility and stability with relative standard deviations lower than 2.01%. It was also applied to determine synephrine in the extract of *Citrus aurantium* L. with recoveries between 99.0% and 102.0%. The content of synephrine was in good agreement with that of the HPLC method. Based on its convenience and stability, the proposed nafion/UiO-66/GN/SPCE could be further developed as a portable and rapid detection sensor for natural active compounds in food, agricultural, and pharmaceutical fields.

1. Introduction

Synephrine is a kind of alkaloid naturally existing in the *Citrus aurantium* L., whose ripe fruits are proceeded as traditional Chinese medicines called "Zhi-Shi" (Zhao et al., 2021). It has shown various pharmacological effects and has been utilized in the food, cosmetic, and feed industries over the past decades (Yan et al., 2020). Due to the structural similarity with endogenous amine neurotransmitters, synephrine could enhance thermogenesis and fat oxidation, promote appetite, increase blood pressure, and accelerate metabolism (Tette et al., 2017). However, it is also reported that there are some side effects and safety issues, which make the use and dose of synephrine more worrisome and restrictive (Fan et al., 2012). A lot of breeding research is undergoing to cultivate varieties with high synephrine content in our institute and around the world (Denaro et al., 2020). While, the traditional determination of synephrine was primarily based on chromatographic methods including HPLC-DAD, HPLC-MS, UPLC-MS, and GC-MS (Al-Khadhra, 2020). Although the results obtained by these methods were accurate, the processing of the sample was relatively complex and the requirement of equipment for laboratories was high. To meet the needs of modern research, the rapid and simple detection of synephrine in fruits and products is essential for related evaluations (Ruiqing et al., 2019).

As a kind of ultrasensitive detection method, electrochemical sensors for synephrine are attractive to researchers because of their convenience, portability, and sensitivity (Wang et al., 2021; Yan et al., 2022). Through the customizations in size and composition of sensors, in the combination of the designed small and portable workstation, a preliminary and rapid detection of synephrine could be completed in the field, which would save a lot of time and labor in agricultural research (Gu et al., 2022). The screen-printed carbon electrode (SPCE) is a type of inexpensive and versatile sensor. Compared to conventional electrodes, SPCE could be designed and tailored in assorted shapes and sizes according to different demands (Camargo et al., 2021). As the technology developed recently, SPCE shows characteristics like modifiable electrode surface, low analytical volume, adequate reproducibility, and

* Corresponding author.
** Corresponding author.
*** Corresponding author.
E-mail addresses: liuliangliang@caas.cn (L. Liu), duanshengwen@caas.cn (S. Duan), aipingxiao@yahoo.com (A. Xiao).

https://doi.org/10.1016/j.crfs.2022.07.008
Received 23 February 2022; Received in revised form 28 June 2022; Accepted 13 July 2022
Available online 20 July 2022

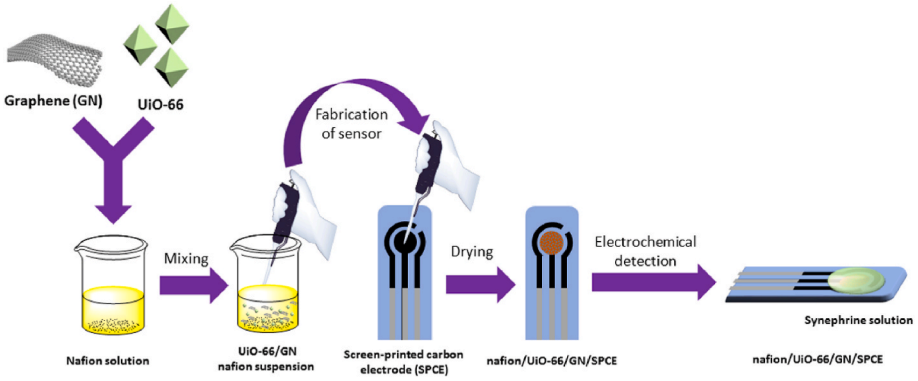

Fig. 1. Scheme of nafion/GN/UiO-66/SPCE and electrochemical detection of synephrine.

accuracy (Suresh et al., 2021). Recently, many types of research using SPCE have been reported to detect DNA, protein, metal ions, pharmaceutical ingredient, and pesticides, exhibiting high potential for commercial applications (Chen et al., 2018; Wang et al., 2018, 2019; Zhang et al., 2019; Fu et al., 2020).

As a typical two-dimensional nanomaterial, graphene (GN) has displayed many properties, including large specific surface areas, high chemical stability, and excellent electrochemical properties (Raghavan et al., 2021). It is widely used to modify electrodes to achieve better results. The modification effects in electrochemical sensors have been proven repeatedly in many years (Jiang et al., 2021). Metal-organic frameworks (MOFs) are a kind of nanomaterials containing organic ligands and metal ions, which exhibit advantages like high surface area, variable porous structure, and controllable composition (Lv et al., 2021). MOFs are widely applied in separation, drug delivery, catalysts, and sensors (Yuan et al., 2018). UiO-66 is a kind of zirconium MOFs with porosity, simple preparation, and high stability, used in catalysis, adsorption, and electrochemical sensor (Du et al., 2019).

Up to now, only a few electrochemical sensors for synephrine are reported using MXene and multi-wall carbon nanotube modified on glassy carbon electrode or boron-doped diamond electrode (Liu et al., 2013; Gao et al., 2020; Haššo et al., 2020). Based on these foundations, many materials are tried in this study to modify the electrode to get higher signals in the electrochemical detection of synephrine, and GN and UiO-66 are finally confirmed for the modifications of SPCE. After characterizing materials, GN and UiO-66 are successively modified on SPCE (UiO-66/GN/SPCE) to develop a novel electrochemical sensor for selective and sensitive detection of synephrine in an aqueous solution. To enhance the adhesion of coatings on the SPCE surface and stabilize the signal, nafion is used as an accessory ingredient in nanomaterial suspension with its chemical inertness and permeability to cations (Patel et al., 2020). With the addition of nafion, GN and UiO-66 are premixed in nafion solution, resulting in the following modification of electrode is only one step (Fig. 1). This modification matches well with the portable sensor and is easier for large-batch production. The composition and fabrication sequence of modifiers are investigated and optimized. Under optimal manufacturing and analytical conditions, the proposed nafion/UiO-66/GN/SPCE demonstrates enhanced electrochemical signals, good linearity, and anti-interference capacity. The content of synephrine in the extract of *Citrus aurantium* L. is detected using the proposed sensor, and the result is compared with the conventional HPLC method. As a result, the nafion/UiO-66/GN/SPCE could be expected to have extensive applications in the detection of natural ingredients.

2. Materials and methods

2.1. Reagents and materials

Graphene (GN) was purchased from Nanjing XFNANO Materials Tech Co., Ltd. (Nanjing, China). (±)-Synephrine (>98.0%), zirconium chloride, 2-aminoterephthalic acid, N,N-Dimethyl formamide (DMF), and acetonitrile in the chromatographic grade were obtained from Macklin Inc. (Shanghai, China). Nafion (5%) was brought from Sigma-Aldrich (St. Louis, MO, USA). Deionized water used in the experiments was supplied by an ELGA water purification system (ELGA Berkefeld, Veolia, Germany). All other chemicals were bought from Sinopharm Chemical Reagent Co., Ltd. (Shanghai, China) with analytical grade. The fruits of *Citrus aurantium* L. were collected from the experimental base belonging to our institute and proceeded according to the guidelines and procedures specified in the Chinese Pharmacopeia 2020 version.

2.2. Instrumentation

The electrochemical measurements were conducted using a CHI 660E electrochemical workstation (Shanghai Chenhua Co., Ltd., China). The screen-printed carbon electrode (SPCE) was purchased from Qingdao Poten Technology Co., Ltd. (Qingdao, China) composed of a carbon working electrode (4 mm diameters), a carbon auxiliary electrode, and an Ag reference electrode. A sensor connector was handmade in the lab and adapted for the workstation. The working electrode would be modified in this study as further described.

The morphology of materials was observed by scanning electron microscope (SEM) on a JSM 6610Lv scanning electron microscopy equipped with an energy dispersive spectroscopy (EDS) detector (JEOL, Tokyo, Japan). The structural analysis of materials was performed by X-ray powder diffraction (XRD) on a RINT 2500 powder X-ray Diffractometer using Cu–K(α) radiation (Rigaku Corporation, Tokyo, Japan). The Fourier transform infrared (FTIR) spectra were recorded on a Vector 22 Fourier transform infrared spectrometer in the range of 400–4000 cm^{-1} (Bruker, German).

HPLC analysis was completed on the Agilent 1260 HPLC, which included a quaternary pump, an autosampler, a thermostatic column compartment, and a diode array detector (Agilent Technologies Inc., Santa Clara, CA, USA). An Agilent ZORBAX C18 column was employed (250 × 4.6 mm i.d.; 5 μm, Santa Clara, CA, USA).

2.3. Preparation of UiO-66

As the previously reported procedure indicated, the UiO-66 was prepared with some modifications (Wang et al., 2020). Typically, 0.54 g of 2-aminoterephthalic acid and 0.50 g of zirconium chloride were mixed in 60 mL of DMF and moved to ultrasonic treatment for 1.0 h. 2.0 mL of hydrochloric acid (10%, v:v) was then added to the mixture to obtain a clear solution. After another 30 min of ultrasonication, the mixture was poured into a Teflon-lined autoclave and reacted at 100 °C for 36 h. When the reaction was complete, and the reactor was cooled, the products were separated by centrifugation and washed with DMF. Finally, the precipitate of UiO-66 was collected and dried in a vacuum

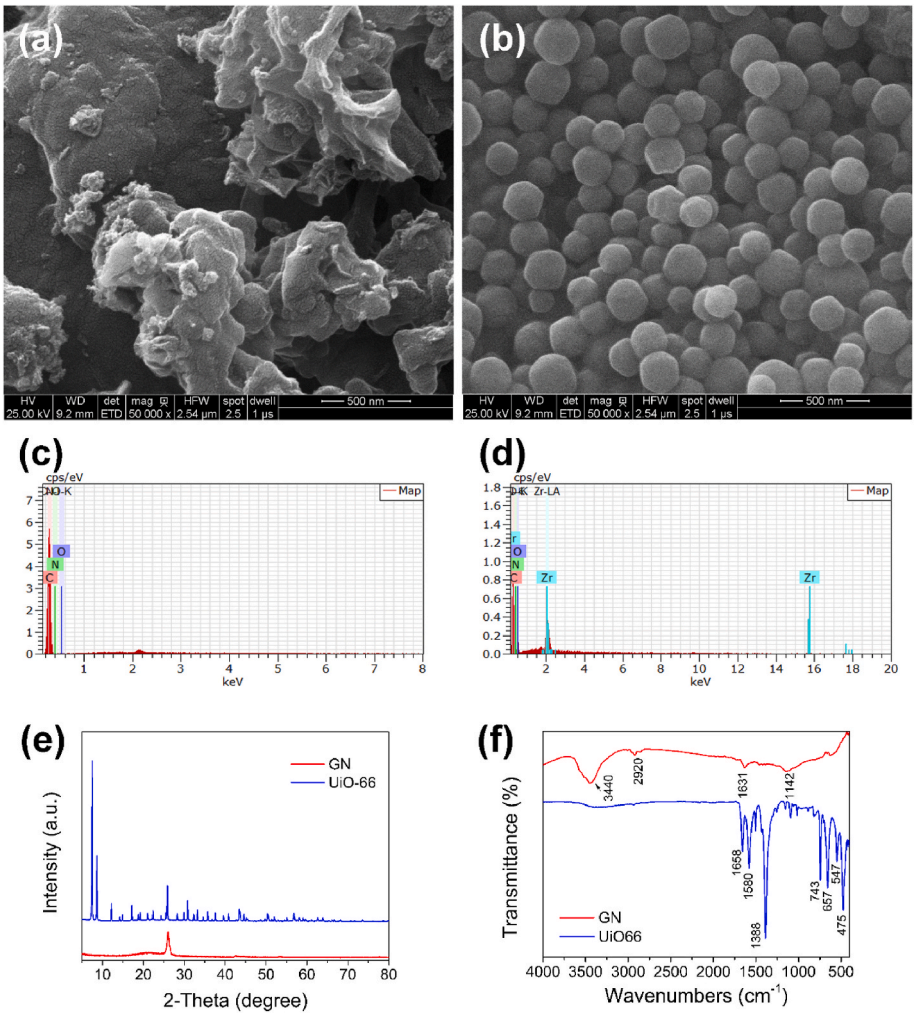

Fig. 2. SEM images of (a) GN and (b) UiO-66. EDS of (c) GN and (d) UiO-66. (e) XRD patterns of GN and UiO-66. (f) FTIR spectra of GN and UiO-66.

for further use.

2.4. Preparation of the modified electrodes

Firstly, the UiO-66/GN nafion suspension was prepared by respectively dispersing 5 mg of UiO-66 and 5 mg of GN in 1 mL of nafion solution (0.5 wt% in 40% ethanol). And then, the mixture was processed in ultrasonication for 30 min to obtain a homogeneous suspension. 8.0 μL of the UiO-66/GN nafion suspension was gently dropped on the surface of the carbon working electrode of SPCE and dried in the air to make an active layer. The modified electrode was termed nafion/UiO-66/GN/SPCE. For comparison, the same amount of UiO-66/GN without nafion, UiO-66, and GN was respectively fabricated on SPCE in the same procedures and conditions and designed as UiO-66/GN/SPCE, UiO-66/SPCE, and GN/SPCE.

2.5. Electrochemical measurements

The electrochemical measurements were performed on the SPCE by immersing the SPCE in synephrine solution using phosphate buffer solution (PBS, 10 mmol L^{-1}, pH 7.0) as the solvent and supporting electrolyte. Electrochemical impedance spectroscopy (EIS) was conducted in 5.0 mmol L^{-1} of $K_3[Fe(CN)_6]/K_4[Fe(CN)_6]$ containing 0.1 mol L^{-1} of potassium chloride with the amplitude of 0.005 V and the frequency range from 0.01 to 10^5 Hz. Cyclic voltammetry (CV) was used for the measurements with the scan rate of 0.05 V s^{-1} and the potential range from 0 V to 1.0 V. Linear sweep voltammetry (LSV) was performed for quantitative analysis in the range from 0.4 to 1.0 V. All experiments were carried out in three duplicates at 25 ± 2 °C.

2.6. Detection of real sample

0.5 g of *Citrus aurantium* L. were added to 50 mL of 20% ethanol solutions (v:v), and it was then placed to ultrasonic extraction for 30 min (KQ5200DV, 200 W, Kunshan Ultrasonic Instrument Co., Ltd., Kunshan, China). The transparent extraction was obtained after the centrifugation for 1 min. Before the detection by the proposed sensor, the transparent extraction was diluted 20 times by PBS (10 mmol L^{-1}, pH 7.0).

To confirm the detection results using the proposed sensor, the HPLC method was applied to detect samples (He et al., 2011). The mobile phases were 0.1% formic acid (A) and acetonitrile (B). A gradient elution program was applied at 25 °C as 0–5 min, 10% B; 5–10 min, 10–15% B; 10–30 min, 15–50% B. The flow rate was 1.0 ml/min. The detector was set at 274 nm. The sample was filtrated by a 0.45 μm filter before analysis.

3. Results and discussion

3.1. Characterization of UiO-66 and GN

3.1.1. SEM

The typical SEM images of GN and UiO-66 were investigated and

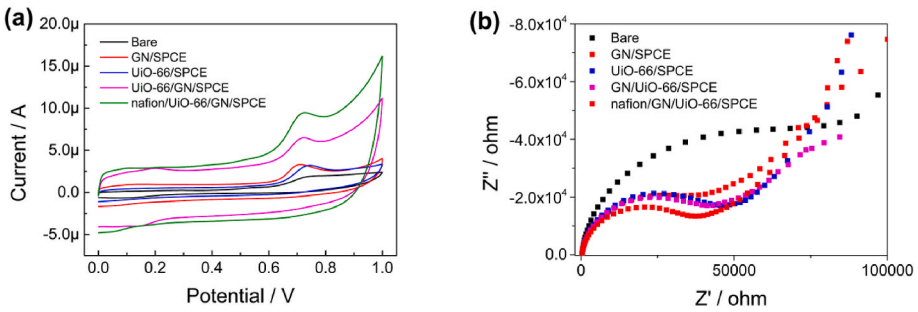

Fig. 3. (a) CV behaviors of synephrine (60 μmol L^{-1}) in PBS (10 mmol L^{-1} pH 7.0) on bare SPCE, GN/SPCE, UiO-66/SPCE, GN/UiO-66/SPCE and nafion/GN/UiO-66/SPCE. Potential range: 0–1.0 V. Scan rate: 50 mV s^{-1}; (b) Nyquist plots of bare SPCE, GN/SPCE, UiO-66/SPCE, GN/UiO-66/SPCE and nafion/GN/UiO-66/SPCE in 5.0 mmol L^{-1} of $K_3[Fe(CN)_6]/K_4[Fe(CN)_6]$ and 0.1 mol L^{-1} of KCl. The amplitude is 0.005 V with a frequency range of 0.01–10^5 Hz.

shown in Fig. 2a and b. The GN possessed a sheet-like structure with a smooth surface and wrinkled edge (Cen et al., 2017). The prepared UiO-66 had a spherical structure with a size distribution between 200 and 250 nm. The typical octahedral structure was not apparent, which might be due to the small size (Yao et al., 2020). In addition, SEM-EDS analysis further revealed the presence of C, O, N, and Zr elements in GN and UiO-66 (Fig. 2c and d). The EDS diagram of GN showed the presence of 95.6 at.% of C, 2.4 at.% of N, and 2.0 at.% of O as basic elements (C. Zhang et al., 2021). In comparison, the EDS diagram of UiO-66 indicated that it was composed of C, O, N, and Zr elements. The atomic percentages were 78.8 at.%, 17.7 at.%, 2.5 at.%, and 1.0 at.%, respectively, showing it was successfully prepared (Meng et al., 2020).

3.1.2. XRD

The structural properties of GN and UiO-66 were analyzed by XRD, and the XRD patterns were shown in Fig. 2e. The diffraction peak of GN at $2\theta = 26°$ could be considered as the characteristic reflection from (002) parallel graphene layers (Kulkarni et al., 2014). For prepared UiO-66, the sharp characteristic peaks at $2\theta = 7.5°$, and 8.6° could be observed in the pattern. The showed pattern was in good agreement with that reported in previous literature and the simulated pattern, which demonstrated the excellent crystallinity of UiO-66 (Du et al., 2019). These XRD results confirmed the structures of GN and UiO-66 and assured subsequent uses.

3.1.3. FTIR

The FTIR spectra of GN and UiO-66 were presented in Fig. 2f. The characteristic peak of GN at 3440 cm^{-1} was assigned to the stretching vibration of O–H. The peak at 2920 cm^{-1} was assigned to symmetric vibrations of CH_2 (Zhao et al., 2011). The peaks at 1631 cm^{-1} and 1142 cm^{-1} were designated as the stretching mode of C=C skeletal ring and stretching vibration of C–O alkoxy (Thota et al., 2021). In the spectrum of UiO-66 (Blue line), the peaks at 1658 cm^{-1}, 1580 cm^{-1}, 1388 cm^{-1}, and 743 cm^{-1} were respectively related to the stretching vibration of carboxyl groups, the asymmetric stretching of O–C–O, the symmetric stretching of O–C–O and the O–H bending (Niu et al., 2018; Liu et al., 2021). Moreover, the bands at 657 cm^{-1}, 547 cm^{-1}, and 475 cm^{-1} were assigned to the μ_3-O stretching, Zr-(OC) stretching, and μ_3-OH stretching, respectively (Shangkum et al., 2018).

3.2. Electrochemical behaviors

The electrochemical behaviors of 60 μmol L^{-1} of synephrine at various modified electrodes were monitored and compared with CV in PBS (10 mmol L^{-1}, pH 7.0). As shown in Fig. 3a, there was no obvious peak on bare SPCE (Black line). After the respective modifications of GN and UiO-66 on SPCE, small oxidation peaks at about 0.7 V could be observed on GN/SPCE (Red line) and UiO-66/SPCE(Blue line), which might owe to the electron transfer properties and the good conductivities of GN and UiO-66 (Xu et al., 2020). When both GN and UiO-66 were modified on SPCE, resulting in UiO-66/GN/SPCE, an apparent increase in oxidation current could be found (pink line). The advantages of GN and UiO-66 were combined in the electrochemical detection of synephrine. This kind of enhancement could be found in reports and previous research (Golkhatmi et al., 2021; Swamy et al., 2021). Since nafion was added to the suspension, the formed nafion/UiO-66/GN/SPCE showed a further signal improvement (Green line). As a cation exchanger with a high cation-exchange capacity, the existence of nafion made the attraction of synephrine and the adhesion of materials better (Hamidi and Zarei, 2020). The surfaces of nafion/UiO-66/GN/SPCE and UiO-66/GN/SPCE were observed by SEM as well (Fig. 4). The presence of nafion made the surface of the modified electrode smoother. Since the GN and UiO-66 were premixed in nafion solution, the fabrication of nafion/UiO-66/GN/SPCE was not complicated, and the difficulty of the

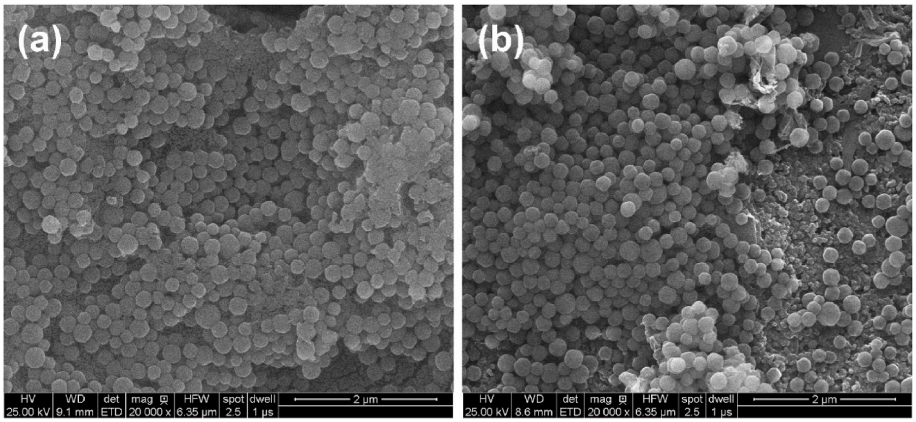

Fig. 4. SEM images of surfaces of (a) nafion/UiO-66/GN/SPCE and (b) UiO-66/GN/SPCE.

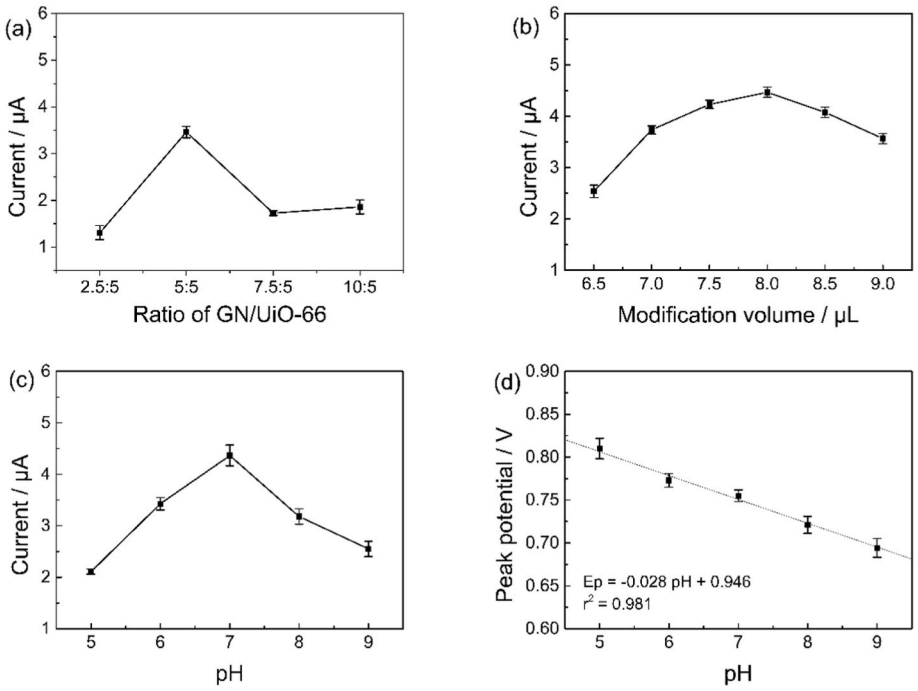

Fig. 5. (a) Effect of Ratio of GN and UiO-66 on peak current in the CV; (b) Effect of modification volumes on peak current in the CV; (c) Effect of pH on peak current in the CV; (d) Plot of peak potential (Ep) to pH values. CV method: 60 μmol L^{-1} of synephrine in 10 mmol L^{-1} of PBS (pH 7.0). Potential range: 0–1.0 V. Scan rate: 50 mV s^{-1}.

experiment was controlled. Consequently, the nafion/UiO-66/GN/SPCE was confirmed as the modifications of the sensor because of the best signal of synephrine in CV detection.

The EIS spectra of sensors were applied to investigate the change of charge transfer resistance (Rct) of modified electrodes. The diameter of the semicircle in the low-frequency part represented the value of Rct in the Nyquist plots (Fig. 3b) (Y. Zhang et al., 2021). It could be found that the semicircle parts of modified electrodes were smaller than that of bare SPCE, which indicated the decreases in resistance after modifications. The Rct of finally nafion/UiO-66/GN/SPCE demonstrated the most decrease, indicating that the GN and UiO-66 improved the conductivity of the sensor in the presence of nafion (Manoj et al., 2022). The effective area of nafion/UiO-66/GN/SPCE could be calculated by the Randles-Sevcik equation ($I_p = 2.69 \times 10^5$ A $D^{1/2}$ $n^{3/2}$ $\upsilon^{1/2}$ C), where A is the effective area of the electrode (cm^2), D is the diffusion coefficient of $K_3[Fe(CN)_6]$ (7.6×10^{-6} cm^2 s^{-1}), n is the transfer number of electrons, υ is the scan rate (V s^{-1}) and C is the concentration of $K_3[Fe(CN)_6]$ (5 mmol L^{-1}). As a result, the effective area of bare SPCE and nafion/UiO-66/GN/SPCE was 0.018 cm^2 and 0.024 cm^2, indicating the increase in the effective area through modification.

3.3. Optimization of assembly and analytical conditions

3.3.1. Ratio of GN and UiO-66

The addition of nafion could keep the nanomaterials from falling off the surface and maintain the level of signals. Then, GN and UiO-66 were first mixed in nafion solution instead of respectively dropping during the sensor modification. To get the optimum composition of the mixture, the ratios of GN and UiO-66 (2.5:5, 5:5, 7.5:5, and 10:5, w:w) were investigated and shown in Fig. 5a. These results suggested that the electrochemical signals of synephrine became the highest when GN and UiO-66 were both in 5.0 mg mL^{-1}. Therefore, the material ratio of GN and UiO-66 was selected as 5:5, which meant 5.0 mg mL^{-1} of GN and UiO-66 were optimal for the fabrication of the electrode.

3.3.2. Modification volumes

The effect of modification volumes of UiO-66/GN nafion suspension was conducted from 6.5 μL to 9.0 μL. As the previous experiment indicated, the concentrations of GN and UiO-66 were set at 5.0 mg mL^{-1}. It could be observed in Fig. 5b that the peak current increased as the volume increased from 6.5 μL to 8.0 μL. However, it began to drop when the volumes continually increased from 8.0 μL to 9.0 μL. Redundant materials on the electrode surface were of no use for the signal of samples in the electrochemical process, which could be supported by previous reports (Fu et al., 2021). Therefore, the modification volume of UiO-66/GN nafion suspension was confirmed at 8.0 μL.

3.3.3. pH of electrolyte

The change in pH value of electrolytes would affect the status of molecules and electrochemical reactions. For this reason, various pH values of electrolytes (5.0, 6.0, 7.0, 8.0, and 9.0) containing samples were prepared using PBS, and the following electrochemical detections were performed by nafion/UiO-66/GN/SPCE in the CV method. The trend was shown in Fig. 5c, and the peak current of synephrine was the highest when the pH value of the electrolyte was 7.0. There were noticeable decreases when the electrolyte became acidic or alkaline, supported by related research (Gao et al., 2020). Thus, 7.0 was adopted as the optimal pH value of electrolytes during tests.

Moreover, it could be observed that there was a linear shift of the peak potential (Ep) to less positive values through the increasing pH values. The linear equation between Ep and pH was expressed as $Ep = -0.028\ pH + 0.946$ ($r^2 = 0.981$) (Fig. 5d). The slope of the equation was about −0.028 V pH^{-1}, which was not similar to the theoretical Nernstian slope of 0.059 V pH^{-1}. This kind of slope implied the electron transfer on the nafion/UiO-66/GN/SPCE might involve two electrons and one proton transfer during the oxidation process, which could be referred to in other research (Manasa et al., 2017; Haššo et al., 2020).

3.4. Influences of scan rate

As an essential parameter reflected the performance of the electrode,

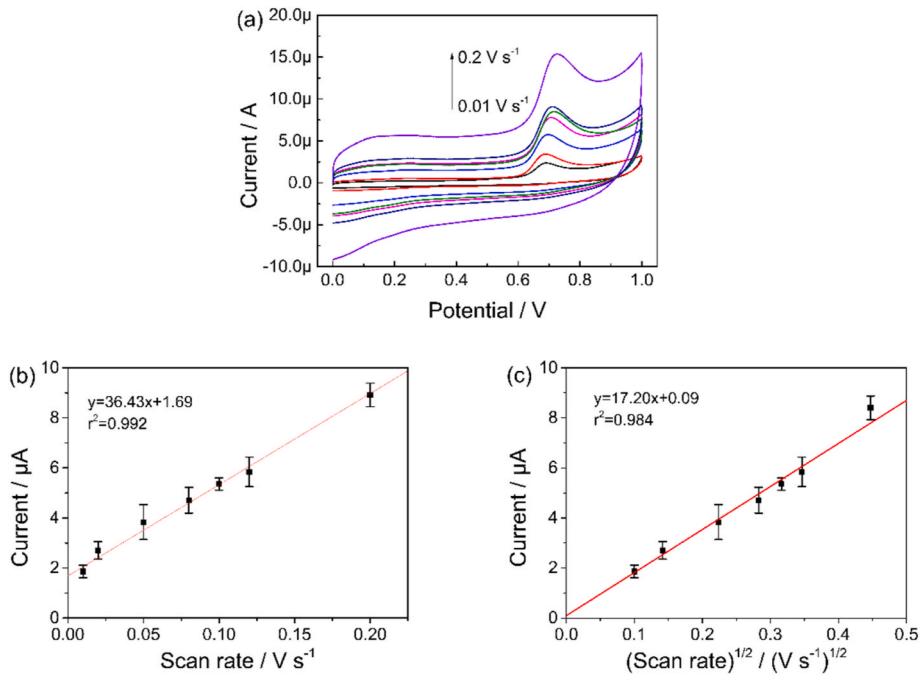

Fig. 6. (a) CV of nafion/GN/UiO-66/SPCE in synephrine solution at different scan rates; (b) The Linear graph of peak currents and scan rates; (c) The Linear graph of peak currents and (scan rates)$^{1/2}$. CV method: 60 μmol L^{-1} of synephrine in 10 mmol L^{-1} of PBS (pH 7.0). Potential range: 0–1.0 V.

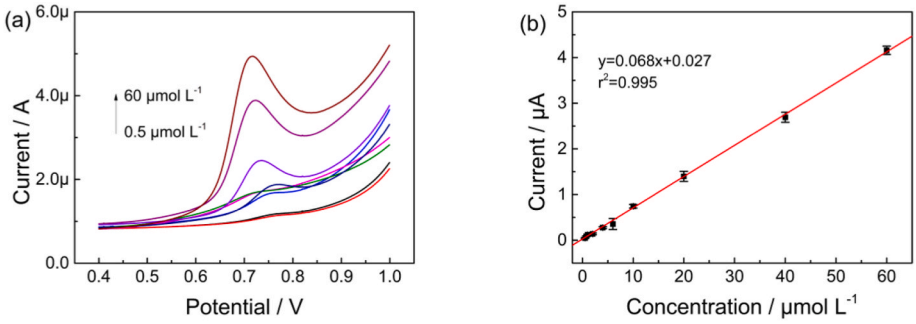

Fig. 7. (a) The LSV of nafion/GN/UiO-66/SPCE in different concentrations of synephrine solutions in 10 mmol L^{-1} of PBS (pH 7.0); (b) Plot of peak current versus concentration of synephrine. LSV method: Potential range: 0.4–1.0 V. Scan rate: 50 mV s^{-1}.

the effect of different scan rates (from 0.01 V s^{-1} to 0.2 V s^{-1}) on the electrochemical response of synephrine in PBS (pH 7.0) was evaluated on nafion/UiO-66/GN/SPCE by CV method. Fig. 6a demonstrated the resulting CV curves at a series of scan rates. It could be found that the peak currents increased and shifted with the increasing scan rates. A linear relationship could be obtained between scan rate and peak current, which would be expressed as Ip = 36.43 v + 1.69 (r^2 = 0.992) (Fig. 6b), indicating the oxidation of synephrine was an adsorption-controlled process (Zhang and Zhang, 2020). Moreover, a linear dependence of peak current against the square root of scan rate ($v^{1/2}$) was observed as well, which was fitted at Ip = 17.20 $v^{1/2}$ + 0.09 (r^2 = 0.984) (Fig. 5c). This trend suggested the electrochemical reaction of synephrine was diffusion-driven (Kesavan et al., 2021).

3.5. Analytical performance of nafion/UiO-66/GN/SPCE for synephrine

To study the quantitative analytical ability of fabricated nafion/UiO-66/GN/SPCE, the LSV curves of synephrine at different concentrations from 0.5 μmol L^{-1} to 60 μmol L^{-1} were observed in PBS (0.01 mol/L, pH 7.0) (Fig. 7a). The results illustrated that the peak current increased with increasing concentrations of synephrine. And a linear dependence could be found between peak current and the concentration of synephrine

Table 1
Comparison of reported sensors for the detection of synephrine.

Electrode	Method	Linear rage (μmol L^{-1})	LOD (μmol L^{-1})	Ref.
–	HPLC	15.25–15250	7.236	Yi et al. (2012)
–	GC-MS	590–299000	590	Marchei et al. (2006)
BDD	DPV	19.6–1000	10.4	Hašško et al. (2020)
	SWV	9.9–1000	8.7	
MWCNTs/ Nafion/GCE	LSV	0.01–10	0.008	Liu et al. (2013)
MXene/ MWCNTs/GCE	LSV	0.5–70	0.167	Gao et al. (2020)
Nafion/UiO-66/ GN/SPCE	LSV	0.5–60	0.04	Present work

BDD: Boron-doped diamond electrode.
MWCNTs: Multi-walled carbon nanotubes.
GCE: Glassy carbon electrode.
DPV: Differential pulse voltammetry.
SWV: Square wave voltammetry.

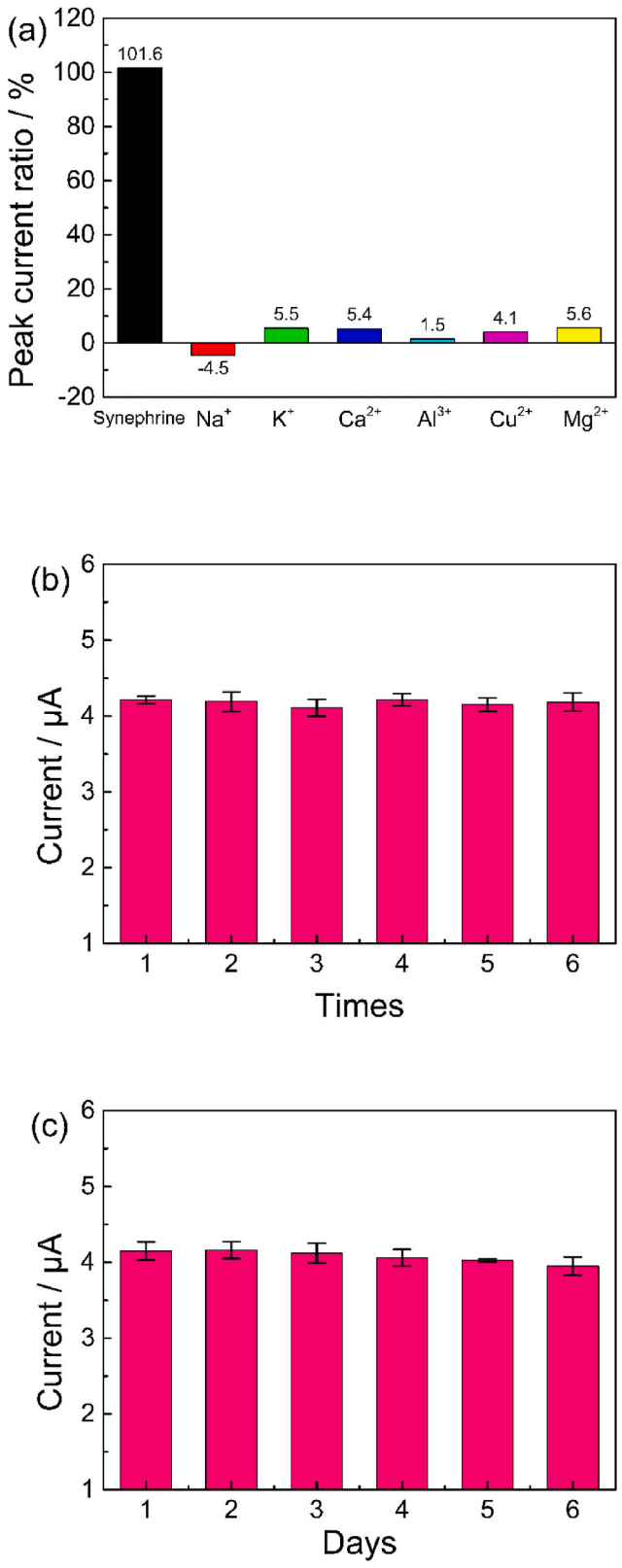

Fig. 8. (a) Peak current ratios of nafion/GN/UiO-66/SPCE in synephrine containing various interfering substances (Na^+, K^+, Ca^{2+}, Al^{3+}, Cu^{2+} and Mg^{2+} ions in 6.0 mmol L^{-1}); (b) Reproducibility of nafion/GN/UiO-66/SPCE in synephrine; (c) Stability of nafion/GN/UiO-66/SPCE in synephrine. LSV method: 60 μmol L^{-1} of synephrine in 10 mmol L^{-1} of PBS. Potential range: 0.4–1.0 V. Scan rate: 50 mV s^{-1}.

during this range, with the detection limit of 0.04 μmol L^{-1} (S/N = 3). Moreover, the limit of quantitation was 0.13 μmol L^{-1} (S/N = 10). The plot of peak current versus concentration of synephrine was shown in Fig. 7b. The regression equation could be expressed as Ip = 0.068 Conc +0.027 (r^2 = 0.995). It demonstrated the quantitative analysis of synephrine using nafion/UiO-66/GN/SPCE was acceptable.

To compare the detection methods for synephrine, the detection abilities of chromatographic methods and reported electrochemical sensors for synephrine were listed in Table 1. Through the comparison, both GC-MS and HPLC methods showed a wide linear range from micromole to millimole. However, electrochemical sensors exhibited good sensitivity, which was the typical advantage of electrochemical technology and could compensate for the shortcomings of traditional technologies (Mokhtar et al., 2022). Among these reported sensors, the proposed nafion/UiO-66/GN/SPCE in this study showed a certain linear detection capability and was adequate for detecting synephrine. Though the proposed sensor in this study was not the most sensitive, the portability and small size derived by SPCE were advantages in the field experiments combined with the use of portable workstations.

3.6. Practical application of nafion/UiO-66/GN/SPCE

3.6.1. Interference study

There are other compounds in the real sample for synephrine analysis, which would become interferences for the intended response. Therefore, the specificity of the fabricated sensor became important in the evaluation of applicability. The selectivity of nafion/UiO-66/GN/SPCE towards synephrine was studied in the presence of interfering inorganic metal ions under optimum conditions. The concentrations of these interfering inorganic metal ions were 100-fold higher than that of synephrine (6.0 mmol L^{-1} to 60.0 μmol L^{-1}). The peak current ratio (%) was introduced as an evaluation indicator, which could be calculated as the proportion of peak current and original peak current variation in the existence of studied interfering inorganic metal ions or targets. As a result, the peak current ratios were shown in Fig. 8a in the respective addition of Na^+, K^+, Ca^{2+}, Al^{3+}, Cu^{2+}, and Mg^{2+} ions, and the same amount of synephrine (60 μmol L^{-1}) was added as a comparison. The peak current ratio of the same amount of synephrine was 101.6%, which showed the used evaluation indicator was sufficient. At the same time, the peak current ratios of interfering ions ranged from 1.5% to 5.6%. According to these results, these interference substances did not interfere with the detection, which demonstrated an acceptable anti-interference ability of the nafion/UiO-66/GN/SPCE.

3.6.2. Reproducibility and stability

The reproducibility of nafion/UiO-66/GN/SPCE in detection was studied by consecutive detection of 60.0 μmol L^{-1} of synephrine six times using the same sensor. During six tests, the fluctuation of peak currents was slight, and the relative standard deviation (RSD) was calculated at 1.0% (Fig. 8b), which showed this fabricated sensor possesses an admissible precision. The stability of nafion/UiO-66/GN/SPCE was also measured by detecting the 60.0 μmol L^{-1} of synephrine on six different days. During the stability test, the sensor was stored in a dry place at room temperature. In the six days of the trial, the peak current remained at 95.2% of the initial value with an RSD of 2.01% (Fig. 8c). The results showed that the nafion/UiO-66/GN/SPCE had good stability

Table 2
Determination of synephrine in the extract of *Citrus aurantium* L. (n = 3).

Samples	Added (μmol L^{-1})	Found (μmol L^{-1})	Recovery (%)	RSD (%)	HPLC (μmol L^{-1})
Extract of *Citrus aurantium* L.	0	26.52	–	2.58	26.91
	10.0	36.72	101.2	1.27	–
	30.0	56.23	99.0	0.76	–

for detection and storage.

3.6.3. Detection of real samples

To check the practicability of the nafion/UiO-66/GN/SPCE in real samples, the extract of *Citrus aurantium* L. was detected. The standard addition method was employed to verify the test results by spiking different amounts of synephrine into samples. The results were presented in Table 2 and compared with the result obtained by the HPLC method. The recoveries during those tests ranged from 99.0% to 102.0%, which indicated the determination of synephrine using the proposed sensor was reliable. The concentration of synephrine was 26.52 μmol L^{-1} compared to 26.91 μmol L^{-1} in the HPLC method. These findings demonstrated that the nafion/UiO-66/GN/SPCE could be sufficiently applied to the samples of natural products.

4. Conclusions

In the present work, a simple nafion/UiO-66/GN/SPCE was fabricated to detect synephrine. The use of GN and UiO-66 improved the electrochemical response of bare SPCE, and the existence of nafion improved the performance of the sensor. The nafion/UiO-66/GN/SPCE displayed quantitative analytical ability for synephrine. Compared to traditional chromatographic methods, the proposed sensor showed advantages in terms of cost, ease of fabrication, and stability, which made the sensor suitable for rapid detection. However, further research on the anti-interference ability in complex samples and stability in long-term use of sensors were still required. With the development of modification materials and assembly strategies, the electrochemical sensors would become a powerful tool in the detection of various active components in the food and pharmaceutical fields.

CRediT authorship contribution statement

Yi Zhang: Data curation, Writing – original draft. **Zongyi You:** Formal analysis, Investigation. **Liangliang Liu:** Methodology, Writing – review & editing. **Shengwen Duan:** Writing – review & editing, Project administration. **Aiping Xiao:** Conceptualization, Project administration.

Declaration of competing interest

The authors declare that they have no known competing financial interests or personal relationships that could have appeared to influence the work reported in this paper.

Acknowledgments

This work was supported by the Chinese Agricultural Science and Technology Innovation Project (No. ASTIP-IBFC05).

References

Al-Khadhra, R.S., 2020. The determination of common anabolic steroid and stimulants in nutritional supplements by hplc-dad and lc-ms. J. Chromatogr. Sci. 58 (4), 355–361. https://doi.org/10.1093/chromsci/bmz121.

Camargo, J.R., Orzari, L.O., Araújo, D.A.G., de Oliveira, P.R., Kalinke, C., Rocha, D.P., Luiz dos Santos, A., Takeuchi, R.M., Munoz, R.A.A., Bonacin, J.A., Janegitz, B.C., 2021. Development of conductive inks for electrochemical sensors and biosensors. Microchem. J. 164, 105998 https://doi.org/10.1016/j.microc.2021.105998.

Cen, Y., Xiao, A.P., Chen, X.Q., Liu, L.L., 2017. Screening and separation of alpha-amylase inhibitors from solanum nigrum with amylase-functionalized magnetic graphene oxide combined with high-speed counter-current chromatography. J. Separ. Sci. 40 (24), 4780–4787. https://doi.org/10.1002/jssc.201700333.

Chen, J., Bai, H., Xia, J., Li, Z., Liu, P., Cao, Q., 2018. Electrochemical sensor for detection of europium based on poly-catechol and ion-imprinted sol-gel film modified screen-printed electrode. J. Electroanal. Chem. 824, 32–38. https://doi.org/10.1016/j.jelechem.2018.07.015.

Denaro, M., Smeriglio, A., Xiao, J., Cornara, L., Burlando, B., Trombetta, D., 2020. New insights into citrus genus: from ancient fruits to new hybrids. Food Frontiers 1 (3), 305–328. https://doi.org/10.1002/fft2.38.

Du, L., Chen, W., Wang, J., Cai, W., Kong, S., Wu, C., 2019. Folic acid-functionalized zirconium metal-organic frameworks based electrochemical impedance biosensor for the cancer cell detection. Sensor. Actuator. B 301, 127073. https://doi.org/10.1016/j.snb.2019.127073.

Fan, J., Zhang, L., Zhang, X., Huang, J., Tong, S., Kong, T., Tian, Z., Zhu, J., 2012. Molecularly imprinted polymers for selective extraction of synephrine from aurantii fructus immaturus. Anal. Bioanal. Chem. 402 (3), 1337–1346. https://doi.org/10.1007/s00216-011-5506-1.

Fu, J., Dong, H., Zhao, Q., Cheng, S., Guo, Y., Sun, X., 2020. Fabrication of refreshable aptasensor based on hydrophobic screen-printed carbon electrode interface. Sci. Total Environ. 712, 136410 https://doi.org/10.1016/j.scitotenv.2019.136410.

Fu, Y., You, Z., Xiao, A., Liu, L., 2021. Magnetic molecularly imprinting polymers, reduced graphene oxide, and zeolitic imidazolate frameworks modified electrochemical sensor for the selective and sensitive detection of catechin. Microchim. Acta 188 (3), 71. https://doi.org/10.1007/s00604-021-04724-1.

Gao, M., Xie, Y., Yang, W.L., Lu, L.M., 2020. Fabrication of novel electrochemical sensor based on mxene/mwcnts composite for sensitive detection of synephrine. Int. J. Electrochem. Sci. 15 (5), 4619–4630. https://doi.org/10.20964/2020.05.79.

Golkhatmi, S.Z., Sedghi, A., Miankushki, H.N., Khalaj, M., 2021. Structural properties and supercapacitive performance evaluation of the nickel oxide/graphene/polypyrrole hybrid ternary nanocomposite in aqueous and organic electrolytes. Energy 214, 118950. https://doi.org/10.1016/j.energy.2020.118950.

Gu, Y., Li, Y., Ren, D., Sun, L., Zhuang, Y., Yi, L., Wang, S., 2022. Recent advances in nanomaterial-assisted electrochemical sensors for food safety analysis. Food Frontiers. https://doi.org/10.1002/fft2.143 n/a(n/a).

Hamidi, M., Zarei, K., 2020. Electrochemical determination of theophylline on a glassy carbon electrode modified with reduced graphene oxide-sodium dodecyl sulfate-nafion composite film. Russ. Chem. Bull. 69 (11), 2107–2112. https://doi.org/10.1007/s11172-020-3007-0.

Haššo, M., Sarakhman, O., Stanković, D.M., Švorc, Ľ., 2020. A new voltammetric platform for reliable determination of the sport performance-enhancing stimulant synephrine in dietary supplements using a boron-doped diamond electrode. Anal. Methods 12 (39), 4749–4758. https://doi.org/10.1039/D0AY01425G.

He, D., Shan, Y., Wu, Y., Liu, G., Chen, B., Yao, S., 2011. Simultaneous determination of flavanones, hydroxycinnamic acids and alkaloids in citrus fruits by hplc-dad–esi/ms. Food Chem. 127 (2), 880–885. https://doi.org/10.1016/j.foodchem.2010.12.109.

Jiang, W., Huang, L.H., Zhang, D.L., Wang, Y., Pan, G.Y., 2021. Graphene-based composites for electrochemical sensor fabrication and their application for drug detection. Int. J. Electrochem. Sci. 16 (3), 13. https://doi.org/10.20964/2021.03.69.

Kesavan, G., Vinothkumar, V., Chen, S.-M., 2021. Sonochemical synthesis of copper vanadate nanoparticles for the highly selective voltammetric detection of antibiotic drug ornidazole. J. Alloys Compd. 867, 159019 https://doi.org/10.1016/j.jallcom.2021.159019.

Kulkarni, S.B., Patil, U.M., Shackery, I., Sohn, J.S., Lee, S., Park, B., Jun, S., 2014. High-performance supercapacitor electrode based on a polyaniline nanofibers/3d graphene framework as an efficient charge transporter. J. Mater. Chem. A 2 (14), 4989–4998. https://doi.org/10.1039/C3TA14959E.

Liu, B., Li, Z., Li, D., Sun, H., Yao, J., 2021. Polyzwitterion-grafted uio-66-pei incorporating polyimide membrane for high efficiency co2/ch4 separation. Separ. Purif. Technol. 267, 118617 https://doi.org/10.1016/j.seppur.2021.118617.

Liu, J., Zhang, W., Li, Y., Yang, L., Ye, B., 2013. A highly sensitive sensor for synephrine detection based on multi-walled carbon nanotubes modified glass carbon electrodes. Anal. Methods 5 (19), 5317–5323. https://doi.org/10.1039/C3AY40830B.

Lv, M., Zhou, W., Tavakoli, H., Bautista, C., Xia, J., Wang, Z., Li, X., 2021. Aptamer-functionalized metal-organic frameworks (mofs) for biosensing. Biosens. Bioelectron. 176, 112947 https://doi.org/10.1016/j.bios.2020.112947.

Manasa, G., Mascarenhas, R.J., Satpati, A.K., D'Souza, O.J., Dhason, A., 2017. Facile preparation of poly(methylene blue) modified carbon paste electrode for the detection and quantification of catechin. Mater. Sci. Eng. C 73, 552–561. https://doi.org/10.1016/j.msec.2016.12.114.

Manoj, D., Rajendran, S., Hoang, T.K.A., Soto-Moscoso, M., 2022. The role of mof based nanocomposites in the detection of phenolic compounds for environmental remediation- a review. Chemosphere 300, 134516. https://doi.org/10.1016/j.chemosphere.2022.134516.

Marchei, E., Pichini, S., Pacifici, R., Pellegrini, M., Zuccaro, P., 2006. A rapid and simple procedure for the determination of synephrine in dietary supplements by gas chromatography-mass spectrometry. J. Pharm. Biomed. Anal. 41 (4), 1468–1472. https://doi.org/10.1016/j.jpba.2006.03.035.

Meng, T., Shang, N., Nsabimana, A., Ye, H., Wang, H., Wang, C., Zhang, Y., 2020. An enzyme-free electrochemical biosensor based on target-catalytic hairpin assembly and pd@uio-66 for the ultrasensitive detection of microrna-21. Anal. Chim. Acta 1138, 59–68. https://doi.org/10.1016/j.aca.2020.09.022.

Mokhtar, N.A.I.M., Zawawi, R.M., Khairul, W.M., Yusof, N.A., 2022. Electrochemical and optical sensors made of composites of metal–organic frameworks and carbon-based materials. A review. Environ. Chem. Lett. https://doi.org/10.1007/s10311-022-01403-2.

Niu, Z., Guan, Q., Shi, Y., Chen, Y., Chen, Q., Kong, Z., Ning, P., Tian, S., Miao, R., 2018. A lithium-modified zirconium-based metal organic framework (uio-66) for efficient co2 adsorption. New J. Chem. 42 (24), 19764–19770. https://doi.org/10.1039/C8NJ04945A.

Patel, B.R., Imran, S., Ye, W., Weng, H., Noroozifar, M., Kerman, K., 2020. Simultaneous voltammetric detection of six biomolecules using a nanocomposite of titanium dioxide nanorods with multi-walled carbon nanotubes. Electrochim. Acta 362, 137094. https://doi.org/10.1016/j.electacta.2020.137094.

Raghavan, V.S., O'Driscoll, B., Bloor, J.M., Li, B., Katare, P., Sethi, J., Gorthi, S.S., Jenkins, D., 2021. Emerging graphene-based sensors for the detection of food

adulterants and toxicants – a review. Food Chem. 355, 129547 https://doi.org/10.1016/j.foodchem.2021.129547.

Ruiqing, L., Te, L., Lihui, W., Shuyun, S., 2019. Synthesis of cdte quantum dots-based imprinting fluorescent nanosensor for highly specific and sensitive determination of caffeic acid in apple juices. eFood 1 (2), 165–172. https://doi.org/10.2991/efood.k.190802.003.

Shangkum, G.Y., Chammingkwan, P., Trinh, D.X., Taniike, T., 2018. Design of a semi-continuous selective layer based on deposition of uio-66 nanoparticles for nanofiltration. Membranes 8 (4). https://doi.org/10.3390/membranes8040129.

Suresh, R.R., Lakshmanakumar, M., Arockia Jayalatha, J.B.B., Rajan, K.S., Sethuraman, S., Krishnan, U.M., Rayappan, J.B.B., 2021. Fabrication of screen-printed electrodes: opportunities and challenges. J. Mater. Sci. 56 (15), 8951–9006. https://doi.org/10.1007/s10853-020-05499-1.

Swamy, N.K., Mohana, K.N.S., Hegde, M.B., Madhusudana, A.M., Rajitha, K., Nayak, S. R., 2021. Fabrication of graphene nanoribbon-based enzyme-free electrochemical sensor for the sensitive and selective analysis of rutin in tablets. J. Appl. Electrochem. 51 (7), 1047–1057. https://doi.org/10.1007/s10800-021-01557-x.

Tette, P.A.S., Guidi, L.R., Bastos, E.M.A.F., Fernandes, C., Gloria, M.B.A., 2017. Synephrine – a potential biomarker for orange honey authenticity. Food Chem. 229, 527–533. https://doi.org/10.1016/j.foodchem.2017.02.108.

Thota, A., Wang, Q., Liu, P., Jian, Z., 2021. Highly electrochemical active composites based on capacitive graphene/aniline oligomer hybrid for high-performance sustainable energy storage devices. Electrochim. Acta 368, 137587. https://doi.org/10.1016/j.electacta.2020.137587.

Wang, Q., Gu, C., Fu, Y., Liu, L., Xie, Y., 2020. Ultrasensitive electrochemical sensor for luteolin based on zirconium metal-organic framework uio-66/reduced graphene oxide composite modified glass carbon electrode. Molecules 25 (19). https://doi.org/10.3390/molecules25194557.

Wang, X., Su, J., Zeng, D., Liu, G., Liu, L., Xu, Y., Wang, C., Liu, X., Wang, L., Mi, X., 2019. Gold nano-flowers (au nfs) modified screen-printed carbon electrode electrochemical biosensor for label-free and quantitative detection of glycated hemoglobin. Talanta 201, 119–125. https://doi.org/10.1016/j.talanta.2019.03.100.

Wang, X., Wang, Y., Shan, Y., Jiang, M., Jin, X., Gong, M., Xu, J., 2018. A novel and sensitive electrogenerated chemiluminescence biosensor for detection of p16ink4a gene based on the functional paste-like nanofibers composites-modified screen-printed carbon electrode. J. Electroanal. Chem. 823, 368–377. https://doi.org/10.1016/j.jelechem.2018.06.030.

Wang, Y., Ma, X., Qiao, X., Yang, P., Sheng, Q., Zhou, M., Yue, T., 2021. Perspectives for recognition and rapid detection of foodborne pathogenic bacteria based on electrochemical sensors. eFood 2 (3), 125–139. https://doi.org/10.2991/efood.k.210621.001.

Xu, L., Li, J., Zhang, J., Sun, J., Gan, T., Liu, Y., 2020. A disposable molecularly imprinted electrochemical sensor for the ultra-trace detection of the organophosphorus insecticide phosalone employing monodisperse pt-doped uio-66 for signal amplification. Analyst 145 (9), 3245–3256. https://doi.org/10.1039/D0AN00278J.

Yan, X., Chen, H., Du, G., Guo, Q., Yuan, Y., Yue, T., 2022. Recent trends in fluorescent aptasensors for mycotoxin detection in food: principles, constituted elements, types, and applications. Food Frontiers. https://doi.org/10.1002/fft2.144 n/a(n/a).

Yan, Y., Zhou, H., Wu, C., Feng, X., Han, C., Chen, H., Liu, Y., Li, Y., 2020. Ultrasound-assisted aqueous two-phase extraction of synephrine, naringin, and neohesperidin from citrus aurantium l. Fruitlets. Prep. Biochem. Biotechnol. 1–12. https://doi.org/10.1080/10826068.2020.1858427.

Yao, X., Shen, J., Liu, Q., Fa, H., Yang, M., Hou, C., 2020. A novel electrochemical aptasensor for the sensitive detection of kanamycin based on uio-66-nh2/mca/mwcnt@rgonr nanocomposites. Anal. Methods 12 (41), 4967–4976. https://doi.org/10.1039/D0AY01503B.

Yi, Y.-N., Cheng, X.-M., Liu, L.-A., Hu, G.-Y., Wang, Z.-T., Deng, Y.-D., Huang, K.-L., Cai, G.-X., Wang, C.-H., 2012. Simultaneous determination of synephrine, arecoline, and norisoboldine in Chinese patent medicine si-mo-tang oral liquid preparation by strong cation exchange high performance liquid chromatography. Pharm. Biol. 50 (7), 832–838. https://doi.org/10.3109/13880209.2011.637505.

Yuan, S., Feng, L., Wang, K., Pang, J., Bosch, M., Lollar, C., Sun, Y., Qin, J., Yang, X., Zhang, P., Wang, Q., Zou, L., Zhang, Y., Zhang, L., Fang, Y., Li, J., Zhou, H.-C., 2018. Stable metal–organic frameworks: design, synthesis, and applications. Adv. Mater. 30 (37), 1704303 https://doi.org/10.1002/adma.201704303.

Zhang, C., Xie, A., Zhang, W., Chang, J., Liu, C., Gu, L., Duo, X., Pan, F., Luo, S., 2021. Cumn2o4 spinel anchored on graphene nanosheets as a novel electrode material for supercapacitor. J. Energy Storage 34, 102181. https://doi.org/10.1016/j.est.2020.102181.

Zhang, J., Zhang, X., 2020. Electrode material fabricated by loading cerium oxide nanoparticles on reduced graphene oxide and its application in electrochemical sensor for tryptophan. J. Alloys Compd. 842, 155934 https://doi.org/10.1016/j.jallcom.2020.155934.

Zhang, Y., Jiang, X., Zhang, J., Zhang, H., Li, Y., 2019. Simultaneous voltammetric determination of acetaminophen and isoniazid using mxene modified screen-printed electrode. Biosens. Bioelectron. 130, 315–321. https://doi.org/10.1016/j.bios.2019.01.043.

Zhang, Y., You, Z., Hou, C., Liu, L., Xiao, A., 2021. An electrochemical sensor based on amino magnetic nanoparticle-decorated graphene for detection of cannabidiol. Nanomaterials 11 (9). https://doi.org/10.3390/nano11092227.

Zhao, S., Wang, X., Sun, W., Gong, X., Yan, J., Tong, S., 2021. Application of liquid-liquid chromatography as a sample pretreatment method for quantitative analysis of synephrine in fructus aurantii immaturus. J. Liq. Chromatogr. Relat. Technol. 44 (3–4), 189–196. https://doi.org/10.1080/10826076.2021.1874981.

Zhao, Y., Zhan, L., Tian, J., Nie, S., Ning, Z., 2011. Enhanced electrocatalytic oxidation of methanol on pd/polypyrrole–graphene in alkaline medium. Electrochim. Acta 56 (5), 1967–1972. https://doi.org/10.1016/j.electacta.2010.12.005.